

Copper-rich complexes in irradiated silicon

Cite as: J. Appl. Phys. **136**, 125701 (2024); doi: [10.1063/5.0232388](https://doi.org/10.1063/5.0232388)

Submitted: 7 August 2024 · Accepted: 10 September 2024 ·

Published Online: 24 September 2024

Nikolai Yarykin^{1,a)} and Jörg Weber²

AFFILIATIONS

¹Institute of Microelectronics Technology RAS, 142432 Chernogolovka, Russia²Technische Universität Dresden, 01062 Dresden, Germany^{a)}Author to whom correspondence should be addressed: NAY@iptm.ru

ABSTRACT

Only copper-related deep-level centers are produced by room-temperature MeV-electron irradiation in silicon doped with a high concentration of mobile interstitial copper atoms. In oxygen-lean FZ-Si, the well-known Cu_{PL} centers of four copper atoms show up in the DLTS, Laplace-DLTS, and photoluminescence measurements. In oxygen-rich Cz-Si, two new centers appear due to the irradiation at the expense of the Cu_{PL} defect. Reaction kinetics analysis correlates the new defects with oxygen, copper, and the irradiation-induced vacancy. The new defects are annealed at temperatures of 150–250 °C and, after passing through two more new configurations, are transformed into Cu_{PL}. The strong similarities to Cu_{PL} suggest that all four new defects are Cu_{PL}-like complexes of four copper atoms perturbed by a nearby oxygen.

© 2024 Author(s). All article content, except where otherwise noted, is licensed under a Creative Commons Attribution-NonCommercial-NoDerivs 4.0 International (CC BY-NC-ND) license (<https://creativecommons.org/licenses/by-nc-nd/4.0/>). <https://doi.org/10.1063/5.0232388>

I. INTRODUCTION

Copper contamination of silicon wafers can significantly impair the device yield.¹ The most dangerous are copper-rich Cu₃Si precipitates, which degrade the gate oxide integrity, enhance leakage currents, and decrease minority carrier lifetime.² According to the recent studies, Cu₃Si nucleation requires that some of the interstitially dissolved copper atoms (Cu_i) become substitutional (Cu_s).³ This can occur due to the interaction of Cu_i with the vacancy-type defects: isolated vacancies, divacancies, and vacancy–impurity complexes. Such defects can be created during the technological processes involving the impact of energetic particles, such as ion implantation or plasma etching.

Two different approaches were applied to study the interaction of copper with radiation defects in Si. First, copper was introduced at relatively low temperatures (close to room temperature) into the pre-irradiated wafers in which all mobile primary radiation defects were already incorporated into stable complexes.^{4–8} Another approach was the irradiation of samples already contaminated with copper.^{5,9,10} In both cases, it was concluded that the mobile Cu_i species react with the vacancy–oxygen pairs (VO), which are the most abundant vacancy-type radiation defects. The resulting CuVO complex possesses donor and acceptor levels at $E_v + 0.20$ and $E_v + 0.49$ eV, respectively.⁶ (E_v stands for the top of the valence band.) It was later shown that the CuVO complexes are formed, at least in part, via the metastable CuVO* configuration

with energy levels at $E_v + 0.44$ and $E_v + 0.51$ eV.^{7,8} According to *ab initio* calculations, the CuVO* and CuVO defects correspond to the Cu atom located either outside or inside the vacancy, respectively.^{9,11,12} It is not yet clear whether the CuVO and CuVO* complexes can trap additional copper atoms. A passivation by Cu_i of the divacancy electrical activity was also noted, although no new levels were detected.^{4,8} Most of these experiments were performed on the oxygen-rich Cz-Si wafers. However, the main results are also valid for the Fz-Si with lower oxygen concentration.^{6,13} (Copper interaction with interstitial-type defects^{14,15} will not be discussed in the present paper.)

A quite different reaction proceeds in samples where a high Cu_i concentration is present during the irradiation with energetic particles. The highly mobile Cu_i species attack primary vacancies before they reach their standard sinks (usually oxygen). In a preliminary study,¹⁶ it was shown that in oxygen-lean float-zone silicon (FZ-Si), virtually all vacancies are consumed in the $\text{Cu}_i + V \rightarrow \text{Cu}_s$ reaction. The created substitutional Cu_s atoms trap additional Cu_i species and form the Cu_{PL} defect with the characteristic low-temperature luminescence band with zero-phonon line at 1014 meV.^{17,18} The Cu_{PL} center has been shown to consist of at least four copper atoms,^{19,20} but its specific structure is still under discussion.^{21–23}

In the present work, we study the spectrum of defects created by electron irradiation in Cu_i-doped silicon wafers with different oxygen contents. In oxygen-rich Cz-Si, the primary vacancy has a

07 October 2024 18:27:30

noticeable probability of forming the VO pair even in the presence of a high concentration of mobile Cu_i species. In these samples, complexes with several copper atoms are nucleated by trapping Cu_i at the Cu_s or VO centers. New data on the formation of the Cu_{PL} defect and the Cu_{PL} -like oxygen-related complexes have been obtained. In addition, our experiments confirmed the diffusivity of isolated vacancies at near room temperature, previously obtained by an interpolation of diffusivities, measured at cryogenic and elevated temperatures.²⁴

II. EXPERIMENTAL DETAILS

Two commercially available *p*-type wafers from different suppliers grown by the Czochralski method (Cz-Si) and one FZ-Si wafer were used in this work. The boron concentration was about 10^{15} cm^{-3} in all crystals. The concentration of dissolved oxygen was $(7-9) \times 10^{17}$ and $< 2 \times 10^{16} \text{ cm}^{-3}$ in the Cz- and FZ-grown wafers, respectively. The carbon concentration was below $4 \times 10^{16} \text{ cm}^{-3}$ in all wafers.

Copper was introduced into the initial wafers by annealing in copper-contaminated quartz ampules at 700–750 °C for 20 min. The temperature and time ensured uniform copper distributions throughout the wafers. The annealing was completed by quenching the samples in liquid nitrogen, after which the samples were stored either in liquid nitrogen or at -30°C with short-term heating to room temperature for irradiation, Schottky diode formation, and mounting to the sample holder.

The concentration of Cu_i was determined by recording the capacitance–voltage (CV) characteristics after cooling the reverse-biased Schottky diode down to 150 K, where the Cu_i atoms are immobile.^{14,25} It is seen in Fig. 1 that the Cu_i concentration could be comparable to the boron concentration, although the exact concentration was dependent on the details of the quenching procedure.

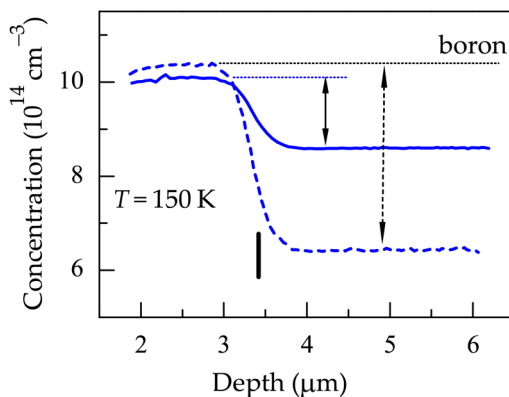


FIG. 1. Active boron depth profiles calculated from the CV characteristics measured in the Cu-doped Cz-Si wafers after cooling from room temperature under the reverse bias of 7 V. The dashed and solid curves correspond to the non-irradiated wafer and to the sample irradiated with $7 \times 10^{14} \text{ cm}^{-2}$ fluence of 5 MeV electrons, respectively. The vertical bar shows the edge position of the space-charge region during cooling. The length of the arrows corresponds to the Cu_i concentrations.

The Cu-doped and as-received wafers were irradiated with 5 MeV electrons at a flux $\sim 5 \times 10^{11} \text{ cm}^{-2} \text{ s}^{-1}$ up to a fluence of 10^{15} cm^{-2} at nominal room temperature. In some cases, the samples were mounted on a water-cooled metal block to avoid overheating during irradiation.

After any irradiation or annealing, all samples were chemically etched in a mixture of nitric and hydrofluoric acids to remove 25–30 μm from the surface. Schottky diodes for electrical measurements were formed by thermal Al evaporation through a shadow mask. Immediately before the evaporation, samples were rinsed in a diluted HF acid. Ohmic contacts were formed on the backside by rubbing-in an eutectic InGa paste.

The deep-level spectra were studied using the standard DLTS and Laplace-DLTS (LDLTS)²⁶ techniques in the temperature range of 35–320 K. The steady-state bias and filling pulse amplitudes were always chosen so that the analyzed layer was located deeper than $\sim 2 \mu\text{m}$ from the surface. Taking into account the deep chemical etching prior to Schottky diode formation and the fact that the maximum penetration depth of hydrogen introduced by etching is less than 1 μm in our samples, the deep level concentrations measured under these conditions correspond to the bulk values.

III. RESULTS

A. DLTS and LDLTS spectra

As a result of copper in-diffusion, practically no deep-level defects were detected in the Cz-Si samples (dashed-dotted curve in Fig. 2). The dominant peak at room temperature is not due to a deep level but due to the presence of mobile Cu_i particles

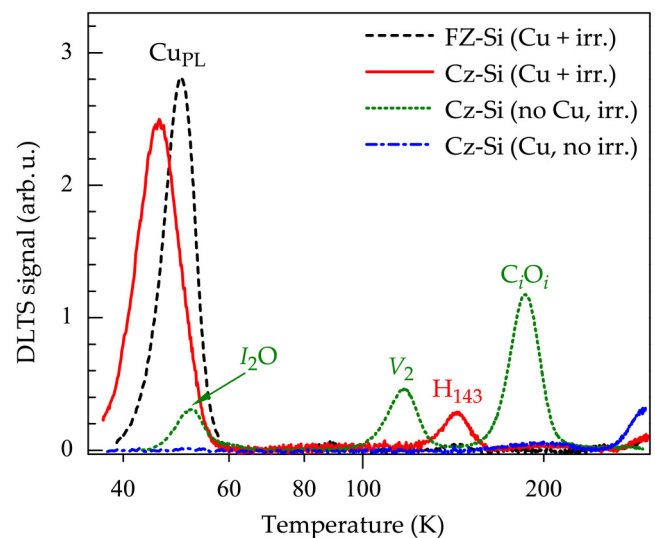


FIG. 2. DLTS spectra of silicon samples irradiated with 10^{15} cm^{-2} fluence of 5 MeV electrons: Cu-doped FZ-Si (dashed curve), Cu-doped Cz-Si (solid curve), and Cu-free Cz-Si (dotted curve). The dashed-dotted curve was measured from the non-irradiated Cu-doped Cz-Si sample. All spectra were taken from layers at 2.1–3.5 μm depths with a 49 s^{-1} rate window. A logarithmic abscissa scale is used to better represent the low-temperature peaks.

07 October 2024 18:27:30

(transient ion diffusion²⁷). A broad peak with a maximum at ~ 200 K is determined by an unidentified defect with concentration $\sim 10^{12} \text{ cm}^{-3}$. The Cu_{PL} centers with the expected DLTS peak at ~ 50 K are practically not detected in Cu-doped Cz-Si (the peak, if any, is at the noise level). In contrast, the Cu_{PL} concentration in FZ-Si samples reached $\sim 10^{13} \text{ cm}^{-3}$ after the same 750°C copper in-diffusion (see Ref. 16). Since the Cu_{PL} defect contains a substitutional copper atom,²⁸ the formation of this defect requires the presence of vacancies. Thus, the difference between Cz-Si and FZ-Si samples is most likely due to the large amount of hidden vacancies in modern FZ-Si that can be released during heat treatment at $\sim 700^\circ\text{C}$.²⁹

The MeV electron irradiation of the wafers with a high concentrations of mobile Cu_i species produces DLTS spectra dominated by low-temperature peaks (dashed and solid curves in Fig. 2). A characteristic feature of these spectra is the absence of peaks related to standard radiation defects known from the literature.^{30,31} (The dotted curve in Fig. 2 shows, on the same scale, the DLTS spectrum measured in the same irradiated Cz-Si material that was not subjected to copper in-diffusion.)

The H_{143} peak of unknown origin appears in some irradiated copper-doped wafers. Despite the similar peak positions, the low thermal stability of the H_{143} center precludes its correlation with the VOH donor.³² This peak will not be discussed further. The increase in DLTS signals at room temperature is due to the presence of mobile Cu_i particles.²⁷

In our preliminary report,¹⁶ the peak at ~ 50 K in FZ-Si was attributed to the donor level of the well-known copper-related Cu_{PL} photoluminescence (PL) center.^{18,33} The identification was based on the DLTS signature and observation of the characteristic PL spectrum in the same samples. In Cz-Si, however, the dominant low-temperature peak is much broader and shifted with respect to Cu_{PL} (solid curve in Fig. 2). This suggests that several different defects contribute to this peak.

Indeed, the LDLTS technique resolves the capacitance relaxation at 46 K into three components (Fig. 3).

The slowest one has the same hole emission rate as the Cu_{PL} center in FZ-Si. The other two components are labeled H_{40} and H_{45} according to the temperature at which they would appear in the DLTS spectrum with a rate window of 49 s^{-1} .

Unlike standard DLTS, the defect concentration in the LDLTS technique is determined not by the amplitude, but by the integral intensity of the peak.²⁶ The vertical lines in Fig. 3 give the calculated concentrations of the corresponding centers. The sum total of the three defects in Cz-Si was always very close to the Cu_{PL} amount in Cu-doped FZ-Si.

In Cz-Si at a given Cu_i concentration, the contribution of Cu_{PL} centers in the low-temperature peak was rather stable in different series of samples. In contrast, the relative concentrations of the H_{40} and H_{45} levels were found to vary significantly with irradiation temperature. H_{40} defects dominate in the samples irradiated at ~ 280 K, while irradiation at higher temperature (310 – 320 K) produces more H_{45} centers.

B. Photoluminescence

Photoluminescence (PL) measurements were performed at 4.2 K in the range of 1060–1600 nm in a semi-quantitative manner.

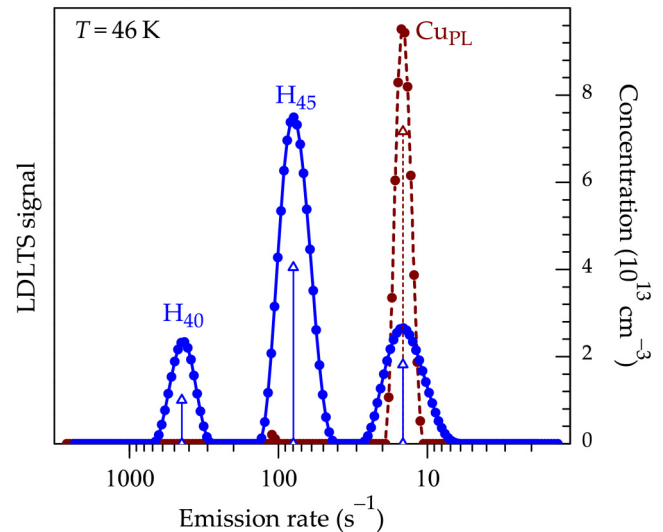


FIG. 3. Laplace-DLTS spectra of Cu-doped Cz-Si (solid curve) and FZ-Si (dashed curve) irradiated with 10^{15} cm^{-2} fluence of 5 MeV electrons. (Note the inverted abscissa scale.) The spectra were taken at 46 K from layers at 2.0–2.3 μm depth under the electric field of 0.7 V/ μm . The concentrations of the observed centers are indicated by the vertical lines with reference to the right scale.

This means that all samples received the same surface treatment and the optical geometry was identical in all cases. As a result, the PL intensity in equivalent samples was reproduced with $\sim 10\%$ accuracy.

All irradiated Cu-doped wafers showed the well-known Cu_{PL} photoluminescence band.¹⁸ No new lines were detected that could be associated with the H_{40} and H_{45} centers. For samples with the same irradiation fluence, the intensity of the Cu_{PL} signal was always proportional to the concentration of the level with the DLTS peak maximum at ~ 50 K. It further confirms that this level belongs to the Cu_{PL} center as shown by Erzgräber and Schmalz.³³ However, in our experiments, the variations of the Cu_{PL} concentration were carried out not by thermal treatments but by different concentrations of the Cu_i species.

C. Electrical parameters of the levels

Arrhenius plots for the H_{40} , H_{45} , and Cu_{PL} traps were measured using the LDLTS technique and are presented in Fig. 4(a). The obtained activation energies and capture cross sections are summarized in Table I.

Another important property of traps is their response to an electric field. The dependences of the hole emission rates R measured by LDLTS at a temperature of 46 K are shown in Fig. 4(b). It is seen that for all three centers the rates depend exponentially on the square of the electric field strength F : $R = R_0 \exp(F^2/F_c^2)$, which is usually interpreted as emission by a phonon-assisted tunneling mechanism.³⁴ The zero-field hole emission rates R_0 and the characteristic electric fields F_c are also given in Table I. The field

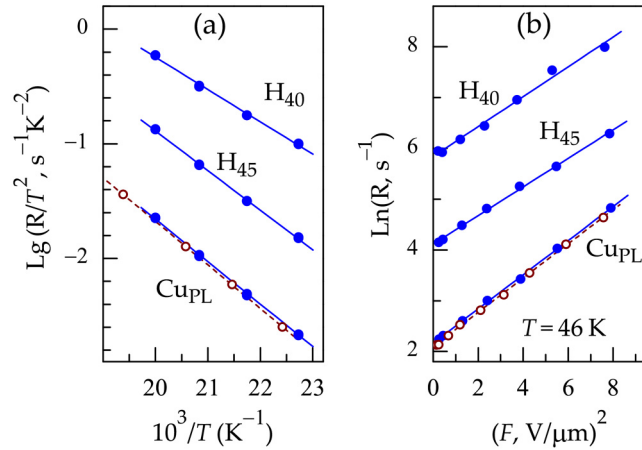


FIG. 4. Arrhenius plots (a) and the dependences of the hole emission rates at 46 K on electric field (b) for the centers measured in the Cu-doped and irradiated samples of Cz-Si (solid symbols) and FZ-Si (circles). Solid and dashed lines are best fits to the data.

dependences of the Cu_{PL} level in Cz-Si and FZ-Si are practically identical. Note that a very close value of $F_c = 1.9 V/\mu m$ was measured at 50 K in the Cu-diffused FZ-Si using the double-DLTS technique (Fig. 3 in Ref. 34).

D. Stability of the H_{40} and H_{45} centers

In the samples with a sufficiently high initial Cu_i concentration, a significant amount of mobile Cu_i particles remains after irradiation (Fig. 1). In particular, the spectra in Fig. 3 were recorded in such samples after cooling the diodes under zero bias, i.e., in the presence of Cu_i species. Alternatively, mobile Cu_i particles can be swept out of the analyzed layer by applying reverse bias at room temperature and cooling the diodes in this state. However, no significant effect of the cooling conditions on the concentrations of the H_{40} , H_{45} , and Cu_{PL} centers was observed. This suggests that all

TABLE I. Parameters of the Cu-related centers: Activation energy E_A , apparent hole capture cross section σ_{app} , zero-field hole emission rate R_0 at 46 K, critical electric field F_c , and level assignment.

| Center | E_A (meV) ^a | σ_{app} ($10^{-16} cm^2$) ^b | R_0 (s^{-1}) | F_c ($V/\mu m$) | Assignment |
|----------------|-----------------------------|--|-----------------------|------------------------|------------|
| Cu_{PL} (Cz) | 75 ± 2 | 2.0 | 8.7 | 1.73 | Cu_4 |
| Cu_{PL} (FZ) | 76 ± 2 | 2.5 | 8.2 | 1.72 | Cu_4 |
| H_{45} | 69 ± 2 | 3.3 | 64 | 1.92 | Cu_4-O |
| H_{40} | 56 ± 3 | 0.8 | 340 | 1.84 | Cu_4-O^* |
| H_{60} | 110 ± 3 | 81 | | | Cu_4-O' |
| H_{70} | 142 ± 2 | 220 | | | Cu_4-O'' |

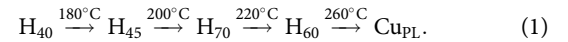
^aUnder average electric field of $0.7 V/\mu m$.

^bCalculated from Arrhenius plots with $v_{th} N_v = 3.3 \times 10^{21} T^2 cm^{-2} s^{-1}$.

three centers are stable against further addition of copper atoms at room temperature.

To test the thermal stability of the H_{40} and H_{45} defects at higher temperatures, the copper-diffused and irradiated Cz-Si wafers were cut into smaller pieces, which were annealed at different temperatures in the range of 150–350 °C for 30 min in air. After annealing, the samples were quickly removed from the furnace and dropped onto a cold metal block. Schottky diodes were formed on the annealed samples after $\sim 30 \mu m$ was removed from the surface by wet chemical etching.

It was found that annealing at 150 °C left the spectrum shown in Fig. 2 with the solid curve virtually unchanged. The DLTS curves measured in the samples annealed at higher temperatures are shown in Fig. 5. Two new peaks with maxima about 70 and 60 K appear and disappear in the annealing temperature interval. (The parameters of the H_{70} and H_{60} levels are also listed in Table I.) The concentration of two new centers seems to be directly correlated with the disappearance of H_{40} and H_{45} . At anneals at 260 °C, only the Cu_{PL} center remains. In general, the transformations of the deep-level spectrum due to annealing can be summarized as follows:



A deconvolution of the measured DLTS spectra allows to determine the defect concentrations after each annealing step. In the first stage, the H_{40} centers were transformed into H_{45} regardless of their initial concentration ratio. Annealing at 180 °C decreases the amount of H_{40} about threefold and its contribution to the

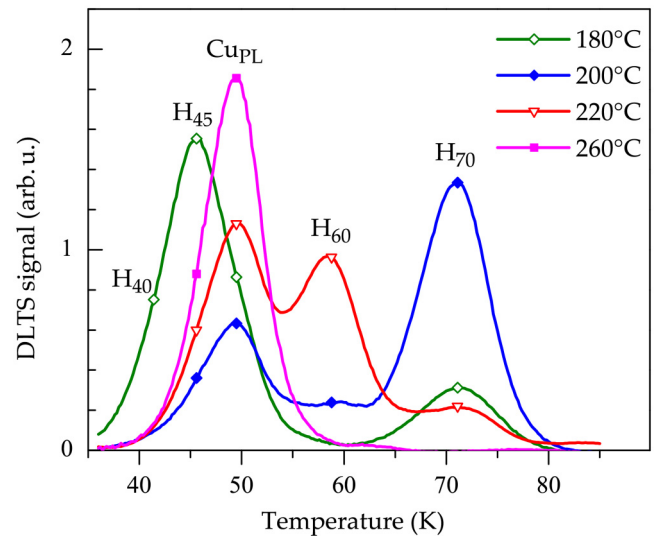


FIG. 5. Low-temperature part of the DLTS spectra in the Cu-doped and irradiated Cz-Si samples annealed at the indicated temperatures for 30 min. The symbols mark the curves and indicate the temperature positions of the corresponding peaks. The spectra were taken from layers at $2.1\text{--}3.5 \mu m$ depths. Rate window is $49 s^{-1}$.

07 October 2024 18:27:30

spectrum shown with the green curve in Fig. 5 was less than 20% compared to H_{45} . In addition, the 180 °C annealing also resulted in the appearance of the H_{70} level, which became dominant after annealing at 200 °C (Fig. 5, blue curve). Further increase of the annealing temperature destroys H_{70} and results in formation of the H_{60} level and the growth of the Cu_{PL} signal (red curve). Finally, only the Cu_{PL} centers remain in the spectrum with a small (<5%) admixture of the H_{45} signal (Fig. 5, magenta curve).

As the temperature increases, the total concentration of all H_{xx} defects gradually decreased and was about 70% and 5% of its initial value after anneals at 220 and 260 °C, respectively. However, the sum total of all H_{xx} and Cu_{PL} was stable under the anneals up to 220 °C with an accuracy better than 10%. Finally, after annealing at 260 °C, this value decreased by ~15%, this loss being partially compensated by the appearance of the Cu_s and $CuVO$ levels at ~100 and 220 K.⁶

In the irradiated samples annealed at 150–180 °C, the concentration of mobile Cu_i species decreased to $(2-3) \times 10^{13} \text{ cm}^{-3}$, which is close to the detection limit of the CV technique. The mobile copper was not detected after annealing at higher temperatures. The appearance of Cu_s and $CuVO$ signals due to annealing at 260 °C indicates that the Cu_i amount was already insufficient to saturate all available traps. To completely remove the Cu_i species and destroy the Cu_{PL} centers, annealing above 300 °C is required.

IV. DISCUSSION

A. Oxygen effects

The Cu_{PL} center is practically the only deep-level defect revealed in our Cu-doped irradiated FZ-Si (Figs. 2 and 3). This defect is formed as a result of Cu_s decoration with Cu_i species.^{28,35,36} Under our experimental conditions, when Cu_s is initially absent, this means that for each Cu_{PL} defect to form, one radiation-induced vacancy must be consumed in reaction with Cu_i . The Cu_{PL} introduction rate in our FZ-Si samples is $0.07 \pm 0.01 \text{ cm}^{-1}$, with the scattering most likely determined by variation of the quenched-in Cu_i concentration.

Due to passivation by Cu_i , divacancies are not detected in the Cu-doped samples.^{4,8} However, assuming that their initial concentration is the same as in Cu-free wafers, we find that the total vacancy introduction rate is $\sim 0.15 \text{ cm}^{-1}$, which is in a good balance with the primary interstitial introduction rate for 5 MeV irradiation in similar crystals (Fig. 7 in Ref. 37). Thus, we conclude that practically all *isolated* vacancies end up as Cu_s in our Cu_i -doped FZ-Si.

The sum total of all three low-temperature peaks in Cz-Si is nearly equal to the Cu_{PL} concentration in FZ-Si (Fig. 3). In accordance with the previous reasoning, one can deduce that all *isolated* vacancies were used to create Cu_{PL} and the novel H_{40} and H_{45} centers. In this sense, the novel centers (as well as Cu_{PL}) are radiation defects of the vacancy type.

The main difference between the studied wafers is a much higher oxygen content in Cz-Si. Therefore, it is reasonable to conclude that the H_{40} and H_{45} centers are related to oxygen. For their generation, some of the primary vacancies should react directly with oxygen (forming the VO pairs), since Cu_s formed by the vacancy interaction with Cu_i is immobile at room temperature and

cannot reach oxygen. The VO pairs are known to bind one Cu_i atom and form the electrically active $CuVO$ and $CuVO^*$ complexes.⁵⁻⁷ However, the levels of these complexes are not seen in Fig. 2.

Considering that the Cu_i species remain in our samples even after irradiation, it can be assumed that the H_{40} and H_{45} centers are formed by trapping additional copper atoms at the $CuVO$ and $CuVO^*$ defects. In this respect, the new centers are Cu-rich defects, similar to the Cu_{PL} center. Since the relative concentration of the H_{40} center increases with lowering the irradiation temperature (Sec. III A), the H_{40} center is most likely related to the metastable $CuVO^*$ defect, while the H_{45} center arises on the basis of $CuVO$.

During annealing, the H_{40}/H_{45} defects transform into Cu_{PL} through a few intermediate states (see Sec. III D). These changes may be associated with a stepwise separation of the oxygen atom. A modeling of the successive transformations (1) gives the activation energies for these processes in the range of 1.5–1.6 eV (with pre-exponential factors of 10^{13} s^{-1}). It is much lower than the energy barrier for oxygen diffusion in bulk, but the barrier could be lowered in the presence of several copper atoms. In this context, it should be recalled that the 300 °C annealing of the $CuVO$ defect, which is essentially the Cu_s-O_i pair, resulted in the appearance of a Cu_s -like center.⁶

The decay of the Cu_{PL} defect is governed by an activation energy of 1.6 eV and pre-exponential factor of $\sim 1.5 \times 10^{13} \text{ s}^{-1}$.^{18,35} This gives the characteristic annealing time of 2 h at 200 °C and only ~2 min at 260 °C. This means that the Cu_{PL} defects observed after the 260 °C annealing for 30 min were formed during the post-annealing cooling because the Cu_i species were still present in the sample during the anneal. Probably, the same conclusion holds for the defects preceding Cu_{PL} in the annealing chain (see Sec. III D).

B. Evaluation of the Cu-rich defect concentrations

Considering the kinetics of vacancy reactions with oxygen and copper, one can estimate the relative formation rates for Cu_{PL} and oxygen-related H_{40} and H_{45} defects during irradiation. The lifetime τ_O of an isolated vacancy with respect to the VO center formation is given by equation

$$\tau_O^{-1} = 4\pi R_O D_V [O_i], \quad (2)$$

where R_O is the distance of the vacancy–oxygen interaction and the square brackets denote the concentration value. An isolated vacancy can be either neutral or doubly positive in p-type Si.³⁸ Estimates show that the majority of vacancies in our moderately doped wafers are neutral at 300 K (the irradiation temperature), and the proportion of positively charged vacancies is negligible even under the electron irradiation conditions. Therefore, taking $R_O = 0.25 \text{ nm}$ and $D_V = 3.3 \times 10^{-11} \text{ cm}^2/\text{s}$ (see Ref. 24), $\tau_O = 120 \text{ ms}$ in our Cz-Si wafers and at least 40 times longer in FZ-Si.

The lifetime τ_{Cu} of an isolated vacancy in terms of conversion to Cu_s is given by equation

$$\tau_{Cu}^{-1} = 4\pi R_{Cu} (D_{Cu} + D_V) [Cu_i], \quad (3)$$

where R_{Cu} is an effective radius of the $V\text{-Cu}_i$ interaction and D_{Cu} is the effective Cu_i diffusivity. The latter accounts for the Cu_i -boron pairing and for our samples $D_{\text{Cu}} = 1.2 \times 10^{-7} \text{ cm}^2/\text{s}$.³⁹ Using $R_{\text{Cu}} = 0.25 \text{ nm}$ and the initial and final Cu_i concentrations from Fig. 1, we find that τ_{Cu} increases during the irradiation from 70 to 200 ms. However, these values can vary significantly from sample to sample due to differences in the quenched Cu_i concentration.

The fraction f_{Cu_i} of isolated vacancies converted to Cu_i and, finally, to Cu_{PL} centers is given by the ratio

$$f_{\text{Cu}_i} = \frac{\tau_{\text{Cu}}^{-1}}{\tau_{\text{Cu}}^{-1} + \tau_{\text{O}}^{-1}}. \quad (4)$$

In the Cu-doped Cz-Si sample shown in Fig. 3, f_{Cu_i} is equal to 0.26, which is in good agreement with the above estimates. This also confirms the assumed room-temperature diffusivity of the vacancy, which was originally deduced from an interpolation of diffusivities measured at cryogenic and elevated temperatures.²⁴

C. Similarities of the Cu-rich defects

Properties of the Cu-rich H_{40} and H_{45} centers are very similar to those of Cu_{PL} . Indeed, the hole emission rates from all these defects show similar activation energies and almost identical dependences on the electric field strength. Furthermore, the thermal stability of the H_{40} and H_{45} centers is comparable to that of Cu_{PL} . This suggests that the structure of the H_{40} and H_{45} centers resembles that of Cu_{PL} , but perturbed by the nearby oxygen atom. The latter may be responsible for the lack of photoluminescence from the oxygen-related defects.

It should be noted, however, that the structure of the Cu_{PL} center remains still unknown. Since this defect was shown to contain at least four copper atoms,^{19,20} the $\text{Cu}_4\text{Cu}_{i3}$ model was developed and the *ab initio* calculations showed that this is the most energetically favorable configuration of the four-Cu clusters considered.^{40,41} However, both the binding energy and the electronic levels calculated for the $\text{Cu}_4\text{Cu}_{i3}$ model^{21,22} are in obvious discrepancy with those experimentally determined for the Cu_{PL} center.

One might suggest that the cluster of four copper atoms calculated in Ref. 41 undergoes some essential rearrangement that turns it into the Cu_{PL} center. Fujimura and Shirai proposed a structure with four copper atoms arranged around a Si vacancy.²³ However, this model contradicts the experimentally observed trigonal symmetry of the Cu_{PL} center¹⁸ and the non-equivalence of the copper atoms.¹⁹ Nevertheless, the above-mentioned similarity between the Cu_{PL} and $\text{H}_{40}/\text{H}_{45}$ centers suggests that the desired transformation also occurs in the copper-rich clusters formed in the vicinity of an oxygen atom.

ACKNOWLEDGMENTS

At the beginning of this work, the studies at TU-Dresden were supported by the Deutsche Forschungsgemeinschaft under Contract No. WE 1319/19. The work at IMT RAS was performed as a part of the State Task No. 075-00296-24-01.

AUTHOR DECLARATIONS

Conflict of Interest

The authors have no conflicts to disclose.

Author Contributions

Nikolai Yarykin: Conceptualization (equal); Formal analysis (equal); Investigation (equal); Writing – original draft (lead). **Jörg Weber:** Conceptualization (equal); Funding acquisition (lead); Investigation (equal); Resources (lead); Supervision (lead); Writing – review & editing (equal).

DATA AVAILABILITY

The data that support the findings of this study are available from the corresponding author upon reasonable request.

REFERENCES

- C. Claeys and E. Simoen, *Metal Impurities in Silicon and Germanium-Based Technologies*, Springer Series in Materials Science Vol. 270 (Springer, 2018).
- A. A. Istratov and E. R. Weber, "Physics of copper in silicon," *J. Electrochem. Soc.* **149**, G21 (2002).
- Y. Ohno, K. Inoue, K. Kutsukake, M. Deura, T. Ohsawa, I. Yonenaga, H. Yoshida, S. Takeda, R. Taniguchi, H. Otubo, S. R. Nishitani, N. Ebisawa, Y. Shimizu, H. Takamizawa, K. Inoue, and Y. Nagai, "Nanoscope mechanism of Cu precipitation at small-angle tilt boundaries in Si," *Phys. Rev. B* **91**, 235315 (2015).
- M. O. Aboelfotoh and B. G. Svensson, "Interaction between copper and point defects in silicon irradiated with 2-MeV electrons," *Phys. Rev. B* **52**, 2522 (1995).
- N. Yarykin and J. Weber, "Interaction of copper impurity with radiation defects in silicon doped with boron," *Semiconductors* **44**, 983 (2010).
- N. Yarykin and J. Weber, "Copper-related deep-level centers in irradiated p-type silicon," *Phys. Rev. B* **83**, 125207 (2011).
- N. Yarykin and J. Weber, "Metastable CuVO^* complex in silicon," *Solid State Phenom.* **205-206**, 255 (2014).
- N. Yarykin and J. Weber, "Radiation defects as probes for the copper and nickel contamination during the chemomechanical polishing of Si wafers," *Mater. Sci. Semicond. Process.* **169**, 107938 (2024).
- V. P. Markevich, A. R. Peaker, I. F. Medvedeva, V. Gusakov, L. I. Murin, and B. G. Svensson, "Radiation-induced defect reactions in Cz-Si crystals contaminated with Cu," *Solid State Phenom.* **131-133**, 363 (2008).
- V. P. Markevich, A. R. Peaker, I. F. Medvedeva, V. E. Gusakov, L. I. Murin, and B. G. Svensson, "Interaction of Cu and Ni impurities with vacancy-related point defects in Czochralski-grown Si crystals," *ECS Trans.* **18**, 1013 (2009).
- D. West, S. K. Estreicher, S. Knack, and J. Weber, "Copper interactions with H, O, and the self-interstitial in silicon," *Phys. Rev. B* **68**, 035210 (2003).
- V. E. Gusakov, in *Proceedings of International Workshop on Radiation Physics of Solid State*, edited by G. G. Bondarenko (Moscow, 2008), p. 642.
- N. Yarykin and J. Weber, "Formation of copper-related deep-level centers in irradiated p-type silicon," *Solid State Phenom.* **178-179**, 154 (2011).
- N. Yarykin and J. Weber, "Interstitial carbon in p-type copper-doped silicon," *Solid State Phenom.* **242**, 302 (2016).
- N. Yarykin, J. Weber, S. Lastovskii, and V. Gusakov, "Copper complexes with carbon-related radiation defects in silicon," *Phys. Status Solidi A* **218**, 2100141 (2021).
- N. Yarykin and J. Weber, "Interaction of interstitial copper with isolated vacancies in silicon," *Solid State Phenom.* **242**, 308 (2016).
- N. S. Minaev, A. V. Mudryi, and V. D. Tkachev, "Radiative recombination at thermal defects in silicon," *Sov. Phys. Semicond.* **13**, 233 (1979).

- ¹⁸J. Weber, H. Bauch, and R. Sauer, "Optical properties of copper in silicon: Excitons bound to isoelectronic copper pairs," *Phys. Rev. B* **25**, 7688 (1982).
- ¹⁹M. L. W. Thewalt, M. Steger, A. Yang, N. Stavrias, M. Cardona, H. Riemann, N. V. Abrosimov, M. F. Churbanov, A. V. Gusev, A. D. Bulanov, I. D. Kovalev, A. K. Kaliteevskii, O. N. Godisov, P. Becker, H.-J. Pohl, J. W. Ager III, and E. E. Haller, "Can highly enriched ^{28}Si reveal new things about old defects?," *Phys. B* **401-402**, 587 (2007).
- ²⁰M. Steger, A. Yang, N. Stavrias, M. L. W. Thewalt, H. Riemann, N. V. Abrosimov, M. F. Churbanov, A. V. Gusev, A. D. Bulanov, I. D. Kovalev, A. K. Kaliteevskii, O. N. Godisov, P. Becker, and H.-J. Pohl, "Reduction of the linewidths of deep luminescence centers in ^{28}Si reveals fingerprints of the isotope constituents," *Phys. Rev. Lett.* **100**, 177402 (2008).
- ²¹A. Sharan, Z. Gui, and A. Janotti, "Hybrid-functional calculations of the copper impurity in silicon," *Phys. Rev. Appl.* **8**, 024023 (2017).
- ²²T. M. Vincent, S. K. Estreicher, J. Weber, V. Kolkovsky, and N. Yarykin, "The Cu photoluminescence defect and the early stages of Cu precipitation in Si," *J. Appl. Phys.* **127**, 085704 (2020).
- ²³T. Fujimura and K. Shirai, "Revisiting the stable structure of the Cu_4 complex in silicon," *Jpn. J. Appl. Phys.* **60**, 021001 (2021).
- ²⁴G. D. Watkins, "The vacancy in silicon: Identical diffusion properties at cryogenic and elevated temperatures," *J. Appl. Phys.* **103**, 106106 (2008).
- ²⁵A. Mesli and T. Heiser, "Defect reactions in copper-diffused and quenched p-type silicon," *Phys. Rev. B* **45**, 11632 (1992).
- ²⁶L. Dobaczewski, A. R. Peaker, and K. Bonde Nielsen, "Laplace-transform deep-level spectroscopy: The technique and its applications to the study of point defects in semiconductors," *J. Appl. Phys.* **96**, 4689 (2004).
- ²⁷T. Heiser and A. Mesli, "Determination of the copper diffusion coefficient in silicon from transient ion-drift," *Appl. Phys. A* **57**, 325 (1993).
- ²⁸H. Lemke, "Störstellenreaktionen bei Cu-dotierten Siliziumkristallen," *Phys. Stat. Sol. A* **95**, 665 (1986).
- ²⁹J. Mullins, V. P. Markevich, M. Vaqueiro-Contreras, N. E. Grant, L. Jensen, J. Jablonski, J. D. Murphy, M. P. Halsall, and A. R. Peaker, "Thermally activated defects in float zone silicon: Effect of nitrogen on the introduction of deep level states," *J. Appl. Phys.* **124**, 035701 (2018).
- ³⁰F. D. Auret and P. N. K. Deenapanray, "Deep level transient spectroscopy of defects in high-energy light-particle irradiated Si," *Crit. Rev. Solid State Mater. Sci.* **29**, 1 (2004).
- ³¹V. P. Markevich, A. R. Peaker, B. Hamilton, V. E. Gusakov, S. B. Lastovskii, L. I. Murin, N. Ganagana, E. V. Monakhov, and B. G. Svensson, "Structure, electronic properties and annealing behavior of di-interstitial-oxygen center in silicon," *Solid State Phenom.* **242**, 290 (2016).
- ³²O. V. Feklisova, N. Yarykin, E. B. Yakimov, and J. Weber, "On the nature of hydrogen-related centers in p-type irradiated silicon," *Phys. B* **308-310**, 210 (2001).
- ³³H. B. Erzgräber and K. Schmalz, "Correlation between the Cu-related luminescent center and a deep level in silicon," *J. Appl. Phys.* **78**, 4066 (1995).
- ³⁴S. D. Ganichev, E. Ziemann, W. Prettl, I. N. Yassievich, A. A. Istratov, and E. R. Weber, "Distinction between the Poole-Frenkel and tunneling models of electric-field-stimulated carrier emission from deep levels in semiconductors," *Phys. Rev. B* **61**, 10361 (2000).
- ³⁵S. D. Brotherton, J. R. Ayres, A. A. Gill, H. W. van Kesteren, and F. J. A. M. Greidanus, "Deep levels of copper in silicon," *J. Appl. Phys.* **62**, 1826 (1987).
- ³⁶N. Yarykin and J. Weber, "Identification of copper-copper and copper-hydrogen complexes in silicon," *Semiconductors* **47**, 275 (2013).
- ³⁷N. Yarykin, O. V. Feklisova, and J. Weber, "Hydrogenation of the dominant interstitial defect in irradiated boron-doped silicon," *Phys. Rev. B* **69**, 045201 (2004).
- ³⁸G. D. Watkins and J. R. Troxell, "Negative-U properties for point defects in silicon," *Phys. Rev. Lett.* **44**, 593 (1980).
- ³⁹A. A. Istratov, C. Flink, H. Hieslmair, E. R. Weber, and T. Heiser, "Intrinsic diffusion coefficient of interstitial copper in silicon," *Phys. Rev. Lett.* **81**, 1243 (1998).
- ⁴⁰K. Shirai, H. Yamaguchi, A. Yanase, and H. Katayama-Yoshida, "A new structure of Cu complex in Si and its photoluminescence," *J. Phys.: Condens. Matter* **21**, 064249 (2009).
- ⁴¹A. Carvalho, D. J. Backlund, and S. K. Estreicher, "Four-copper complexes in Si and the Cu-photoluminescence defect: A first-principles study," *Phys. Rev. B* **84**, 155322 (2011).